Postprint of: Lewandowska J., Szymkiewicz A., Burzyński K., Vauclin M., Modeling of unsaturated water flow in double-porosity soils by the homogenization approach, Advances in Water Resources, Vol. 27, Iss. 3 (2004), pp. 283-296, DOI: 10.1016/j.advwatres.2003.12.004

Modeling of unsaturated water flow in double-porosity soils by the homogenization approach

Jolanta Lewandowska
Laboratoire d'étude des Transferts en Hydrologie et Environnement (LTHE)
(UJF, CNRS, INPG, IRD)
BP53, 38041 Grenoble Cedex 09, FRANCE
jolanta.lewandowska@hmg.inpg.fr

Adam Szymkiewicz
Politechnika Gdańska
Wydział Budownictwa Wodnego i Inżynierii Środowiska
Ulica Narutowicza 11/12
80-952 Gdańsk, POLAND
PhD student at the L.T.H.E. and PG WBWIS

Kazimierz Burzyński
Politechnika Gdańska
Wydział Budownictwa Wodnego i Inżynierii Środowiska
Ulica Narutowicza 11/12
80-952 Gdańsk, POLAND

Michel Vauclin
Laboratoire d'étude des Transferts en Hydrologie et Environnement (LTHE)
(UJF, CNRS, INPG, IRD)
BP53, 38041 Grenoble Cedex 09, FRANCE

ABSTRACT

Double-porosity media are composed of two distinct regions with contrasted hydraulic parameters. Due to this type of structure, transient water flow is characterized by local non-equilibrium conditions. This paper will present a macroscopic model of water flow in such media that was obtained by the method of homogenization. This method enables us to derive the macroscopic model and its effective parameters from a description of the phenomena at the local scale, without any a priori hypothesis for the form of the model. The macroscopic non-equilibrium water flow is described by a single macroscopic equation with a highly non-linear exchange term, leading to a tailing effect. The effective properties, namely the hydraulic conductivity tensor and the specific water capacity, are defined as depending on the hydraulic characteristics of the more conductive (and connected) domain and the local geometry of the medium. A numerical implementation (Fortran program) of the proposed model was developed. Numerical simulations were performed for two different types of geometry. For each problem the results obtained from homogenization are compared with a fine scale numerical simulation where heterogeneous structure of the medium is explicitly represented (SWMS_3D commercial software). Comparisons with the phenomenological approach of Gerke and van Genuchten [14] are also presented.

KEY WORDS:

upscaling, homogenization, unsaturated flow, double-porosity media, non-equilibrium, tailing effect

1. INTRODUCTION

Double-porosity media consist of two interacting sub-domains with contrasted hydraulic properties. One sub-domain corresponds to the porous matrix or soil aggregates, and the other includes inter-aggregate space filled with coarser material, macropores, fractures or fissures which are highly conductive compared to the matrix (Fig. 1). In this type of medium three distinct observation scales can be considered: the microscopic scale (or pore scale), associated with single grains and pores of the medium, the mesoscopic scale (or Darcy scale), which is the scale of a single soil aggregate or porous block and the macroscopic scale, which is of major interest from the point of view of soil hydrology and groundwater modeling. Due to the large contrast in local hydraulic parameters of the soil, non-equilibrium phenomena arise during water flow and contaminant transport, which should be properly taken into account in the mathematical description applied at the macroscale.

Modeling of non-equilibrium flow and transport in unsaturated soils/rocks has received increasing attention during recent years since it concerns such vital problems as protection of groundwater aquifers or securing of waste depositories. A recent review on the subject can be found in Šimůnek et al. [39]. A number of different approaches to modeling the unsaturated flow of water in structured porous media have been developed. They vary from relatively simple single-porosity models to more complicated dual- or multi-porosity/permeability concepts. In the simplest models the heterogeneity of soils is captured by introduction of composite retention and hydraulic conductivity functions into the Richards equation [14,28]. Such single-porosity models account for rapid changes in conductivity when a highly conductive macroporous domain is activated, but they cannot represent non-equilibrium processes between two sub-domains. A simple non-equilibrium flow model was proposed by Ross and Smettem [34] in which an additional kinetic description of the approach of the water content towards equilibrium is added to the Richards equation [33].

The dual porosity phenomenological model was initially suggested by Barenblatt et al. [8], and is widely used in reservoir modeling [7,41]. In this phenomenological approach the regions of high and low permeability are treated as two overlapping continua. The macroscopic model consists of two flow equations: one for each sub-domain. The equations are coupled by a term describing the exchange of water between the two regions. A dual-porosity model for flow and transport in unsaturated soils was presented by Gerke and van Genuchten [15,16]. They assumed that flow in both sub-domains can be simulated by the Richards equation and they proposed a first-order coupling term for water transfer with the difference in pressure heads between the two sub-domains as the driving force, similarly to the model of Barenblatt et al. [8]. The rate of water transfer depends on the local geometry of the medium, which was represented by a geometry dependent coefficient. Gerke and van Genuchten [17] provided values of that coefficient for some simple geometries. For other geometries they suggested a functional relationship between the coefficient and the normalized surface to volume ratio of the matrix aggregates.

Another approach is to use the kinematic wave equation to describe water flow in highly permeable sub-domain, as proposed by Germann [18] and Germann and Beven [19]. The kinematic wave equation was applied in the MACRO model by Jarvis

[24] to simulate macroporous flow, while the flow in soil aggregates was modeled by Richards equation. The rate of water transfer between the two sub domains was assumed to be proportional to the difference in saturations. For porous media that exhibits more than two distinct sub-domains the dual-porosity approach can be extended into multi-porosity models [20].

Alternatively, upscaling (macroscopisation) methods can be used to derive the macroscopic model from the description of physical processes at the local scale, which is the scale of single matrix blocks. The corresponding macroscopic equations can be obtained by different methods. The volume averaging method was applied by Quintard and Whitaker to study one-phase [31] and two-phase [32] equilibrium fluid flow in heterogeneous porous media, while the non-equilibrium model for dispersive transport was presented in [30]. The asymptotic homogenization method has been widely used in recent years to model different flow and transport problems in porous media [22]. For example Saez et al [36] and Amaziane et al [1] studied two-phase equilibrium fluid flow. Macroscopic models of incompressible fluid flow in a dual porosity medium were presented by Arbogast et al. [3], whereas Hornung and Showalter [23] derived dual-porosity transport models. Hornung in [21] applied homogenization to the unsaturated flow and transport in aggregated soils. Application of homogenization theory to obtain macroscopic models of flow and transport in highly heterogeneous porous media was extensively presented in Panfilov in [29]. Lewandowska and Laurent [27] derived a macroscopic model for unsaturated water flow for the conditions of local equilibrium. They applied the physical homogenization approach, proposed by Auriault [5]. This method is based on the analysis of dimensionless numbers which govern the physical processes. The resulting macroscopic models are mathematically and physically rigorous and their domain of validity is precisely defined. The physical homogenization approach was also used to double porosity media by Royer et al. [35], to study highly compressible gas flow in rigid fractured media and incompressible fluid flow in deformable fractured media.

The aims of this paper are as follows: (i) development of a macroscopic model using the homogenization technique, including the following elements: the macroscopic boundary value problem, the definitions of the effective parameters and the local boundary value problem, (ii) definition of the domain of validity of the model, (iii) presentation of the numerical implementation of the mathematical model, (iv) presentation of the results of two numerical simulations, and (v) comparison of the results with other solutions existing in literature.

2. MATHEMATICAL MODEL OF FLOW IN DOUBLE POROSITY SOILS

2.1. General assumptions

We consider a porous medium (soil) that has a double-porosity structure. It is composed of two porous sub-domains of contrasted hydraulic properties. We do not consider fractured media. Let us assume that this medium can be characterized by a representative elementary volume (a REV) [9] or a period, if the medium has a periodic structure. This assumption concerns the scale separation and the existence of an equivalent medium. It is formally written

$$\varepsilon = \frac{l}{L} << 1 \tag{1}$$

where l is the period length (the characteristic microscopic length) and L is the dimension of the macroscopic domain (the characteristic macroscopic length). Without loss of generality we further assume the periodicity of the porous medium and we note Ω the period, Ω_1 and Ω_2 the two porous domains, and Γ the interface between them (Fig. 1). We also assume that the domain Ω_1 is continuously connected and that the porous medium 1 is much better conductive than the porous medium 2.

The unsaturated water flow in a homogenous rigid soil is often described by the Richards equation [32] which assumes that the air pressure in the soil is constant and equal to the atmospheric pressure during the whole flow process. Under isothermal conditions this equation is formulated for the capillary pressure h head [L] being the water pressure head relative to the atmospheric pressure ($h \le 0$) [9] as follows:

$$C(h)\frac{\partial h}{\partial t} - div_{\mathbf{x}}\left(\mathbf{K}(h) grad_{\mathbf{x}}\left(h + X_3\right)\right) = 0 \tag{2}$$

where $C(h) = \frac{d\theta}{dh}$ is the specific water capacity [L^{-1}], θ is the volumetric water content [-], $\mathbf{K}(h)$ is the hydraulic conductivity [$L\ T^{-1}$], the $\mathbf{X} = (X_1, X_2, X_3)$ denotes the physical spatial variable [L], where the axis X_3 is positively oriented upwards and t [T] is the time. Note that in soil physics h represents the potential which is related not only to the capillarity but also to the adsorptive forces [13].
This equation is highly non linear because of the non linear functions $C(h)$ and $K(h)$. Due to the parabolic character of the Richards equation, its behavior as a diffusion equation can be easily viewed as a function of another hydraulic parameter, which is the hydraulic diffusivity $D(h)$ [$L\ T^{-2}$], defined as the ratio of the conductivity over the specific water capacity

$$D(h) = \frac{K(h)}{C(h)} \tag{3}$$

As it can be seen in 2.3, the hydraulic diffusivity $D(h)$ plays a fundamental role in the estimation of the local capillary pressure gradient.

2.2. Formulation of the problem

Since the porous medium presents a double structure, the problem can be regarded at three different scales, namely the pore scale, the Darcy scale and the macroscopic scale. In this paper the starting point of the analysis is the Darcy scale.

Let us assume that in each porous sub-domain the unsaturated water flow can be described locally by the Richards equation

$$C_1 \frac{\partial h_1}{\partial t} - \mathrm{div}_{\mathbf{x}}\left(\mathbf{K}_1 \,\mathrm{grad}_{\mathbf{x}}\left(h_1 + X_3\right)\right) = 0 \qquad \text{in } \Omega_1 \tag{4}$$

$$C_2 \frac{\partial h_2}{\partial t} - \mathrm{div}_{\mathbf{x}}\left(\mathbf{K}_2 \,\mathrm{grad}_{\mathbf{x}}\left(h_2 + X_3\right)\right) = 0 \qquad \text{in } \Omega_2 \tag{5}$$

together with the capillary pressure head and flux continuity conditions at the interface Γ between Ω_1 and Ω_2, written in the form:

$$h_1 = h_2 \qquad \text{on } \Gamma \tag{6}$$

$$\left(\mathbf{K}_1 \,\mathrm{grad}_{\mathbf{x}}\left(h_1 + X_3\right)\right)\mathbf{N} = \left(\mathbf{K}_2 \,\mathrm{grad}_{\mathbf{x}}\left(h_2 + X_3\right)\right)\mathbf{N} \qquad \text{on } \Gamma \tag{7}$$

where h_1 and h_2 are the local capillary water pressures heads, $\mathbf{K}_1(h)$ and $\mathbf{K}_2(h)$ are the hydraulic conductivity tensors, $C_1(h)$and $C_2(h)$are the specific water capacities in Ω_1 and Ω_2, respectively, and **N** is the unit vector normal to Γ. In Eqs. (4) and (5) the X_3 term is related to the gravity. We assume that the water retention curves $\theta_1(h)$ and $\theta_2(h)$, as well as the conductivity curves $\mathbf{K}_1(h)$ and $\mathbf{K}_2(h)$ for each porous sub-domain, are known. In case of hysteresis of $\mathbf{K}(h)$ and $\theta\,(h)$, different functions for drainage and wetting curves respectively can be used.

2.3. Dimensionless variables and estimations of the parameters of the problem

Let us define the dimensionless variables by dividing each variable by its characteristic value. It leads to the following relations

$$h_1 = h_{1C}\, h_1^* \qquad h_2 = h_{2C}\, h_2^* \qquad \mathbf{y} = \frac{\mathbf{X}}{l} \qquad \mathbf{x} = \frac{\mathbf{X}}{L} \qquad t = T\, t^*$$

$$\mathbf{K}_1 = K_{1C}\, \mathbf{K}_1^* \qquad \mathbf{K}_2 = K_{2C}\, \mathbf{K}_2^* \qquad C_1 = C_{1C}\, C_1^* \qquad C_2 = C_{2C}\, C_2^* \tag{8}$$

where the subscript *c* denotes the characteristic quantity (constant) and the asterisk denotes the dimensionless variable. We introduce two space variables:

- $\mathbf{y} = (y_1, y_2, y_3)$ is the microscopic dimensionless space variable,
- $\mathbf{x} = (x_1, x_2, x_3)$ is the macroscopic dimensionless space variable.

T is the characteristic time of observation, chosen to be the time of the water flow in the medium 1 at the macroscopic scale L. Therefore, we can write:

$$T = \frac{C_{1C}\, L^2}{K_{1C}} = \frac{L^2}{D_{1C}} \tag{9}$$

In order to capture the double porosity effect and the resulting non-equilibrium, we assume that the characteristic values of the hydraulic parameters are very contrasted. In particular, we assume that the ratio of the hydraulic diffusivities is of the order $\mathrm{O}(\varepsilon^2)$

$$\frac{D_{2C}}{D_{1C}} = \frac{K_{2C}}{C_{2C}} \frac{C_{1C}}{K_{1C}} = \mathrm{O}\left(\varepsilon^2\right) \tag{10}$$

According to the relation (10), we can examine for example three different combinations of the ratio of the parameters *K* and *C* in the medium 1 and 2:

- $\frac{K_{2C}}{K_{1C}} = \mathrm{O}\left(\varepsilon^2\right)$ and $\frac{C_{1C}}{C_{2C}} = \mathrm{O}(1)$ (11)
- $\frac{K_{2C}}{K_{1C}} = \mathrm{O}\left(\varepsilon\right)$ and $\frac{C_{1C}}{C_{2C}} = \mathrm{O}\left(\varepsilon\right)$ (12)
- $\frac{K_{2C}}{K_{1C}} = \mathrm{O}(1)$ and $\frac{C_{1C}}{C_{2C}} = \mathrm{O}\left(\varepsilon^2\right)$ (13)

Note that the three combinations of the parameters have the same final effect on the macroscopic behavior since they lead to the same estimation of the local capillary head gradients on the interface Γ.
Finally, we can notice that the ratio of characteristic length of the period *l* to the characteristic capillary pressure head h_c is of the order $\mathrm{O}\left(\varepsilon\right)$ in a period. It means that the capillary term is dominating over the gravity one.

2.5. Formulation of the problem for the dimensionless variables

By introducing the dimensionless variables, Eqs. (8), and by taking into account the parameter estimations, the local problem Eqs. (4)-(7) normalized with respect to *l* is written as:

$$\varepsilon^2 C_1^* \frac{\partial h_1^*}{\partial t^*} - \mathrm{div}_{\mathbf{y}}\left(\mathbf{K_1^*}\,\mathrm{grad}_{\mathbf{y}}\left(h_1^* + \varepsilon\, \mathrm{y}_3\right)\right) = 0 \qquad \text{in } \Omega_1 \tag{14}$$

$$C_2^* \frac{\partial h_2^*}{\partial t^*} - \mathrm{div}_{\mathbf{y}}\left(\mathbf{K_2^*}\,\mathrm{grad}_{\mathbf{y}}\left(h_2^* + \varepsilon\, \mathrm{y}_3\right)\right) = 0 \qquad \text{in } \Omega_2 \tag{15}$$

$$h_1^* = h_2^* \qquad \text{on } \Gamma \tag{16}$$

$$\left(\mathbf{K}_1^*\,\mathrm{grad}_{\mathbf{y}}\left(h_1^* + \varepsilon\, \mathrm{y}_3\right)\right)\mathbf{N} = \varepsilon^2 \left(\mathbf{K_2^*}\,\mathrm{grad}_{\mathbf{y}}\left(h_2^* + \varepsilon\, \mathrm{y}_3\right)\right)\mathbf{N} \qquad \text{on } \Gamma \tag{17}$$

Note that all the terms in the problem (14) - (17) are of the order O(1). The factor ε^2 in Eqs (14) and (17), comes from the contrast between the hydraulic properties of the two materials.

2.4. Homogenization

In this study, the classical method of homogenization by formal asymptotic expansions was applied [10,37]. The formalism has been recently extensively developed, in particular for the applications to the non-linear problems (see for example [6]). The procedure adopted in this paper was presented in details by Auriault [4,5]. The homogenization postulates that all the unknowns ϕ

(dimensionless) can be presented in form of an asymptotic expansion:

$$\phi(\mathbf{x},\mathbf{y},t^*) = \phi^{(0)}(\mathbf{x},\mathbf{y},t^*) + \varepsilon\phi^{(1)}(\mathbf{x},\mathbf{y},t^*) + \varepsilon^2\phi^{(2)}(\mathbf{x},\mathbf{y},t^*) + \ldots \tag{18}$$

where $\phi(\mathbf{x},\mathbf{y},t^*)$ stands for h_1^*, h_2^*, C_1^*, C_2^*, K_1^*, K_2^*, θ_1^* or θ_2^*. Note that all the terms $\phi^{(i)}(\mathbf{x},\mathbf{y},t^*)$ in Eq. (18) are dimensionless. Due to the scale separation the unknowns $\phi^{(i)}$ are functions of three variables: **x**, **y** and t^*, where we have $\mathbf{x} = \varepsilon\mathbf{y}$. The derivation operator is written:

$$\frac{\partial}{\partial \mathbf{y}} \mapsto \frac{\partial}{\partial \mathbf{y}} + \varepsilon\frac{\partial}{\partial \mathbf{x}} \tag{19}$$

In the case considered here the periodicity of the problem implies that $h^{(i)}$, $C^{(i)}$, $K^{(i)}$ and $\theta^{(i)}$ in both sub-domains are **y**-periodic. The strategy of homogenization involves three main steps: (i) introducing the expansion (18) into the problem (14)-(17); (ii) identification of the problems at the same powers of ε; and (iii) solving the successive order boundary value problems within the period domain. Herein we present the main results of homogenization, without formal demonstration of existence and uniqueness of the solution of each problem.

2.5. Macroscopic variable $h_1^{(0)}$

In order to analyze the behavior of the macroscopic variable $h_1^{(0)}$ we rewrite Eqs (14) and (17) at the power ε^0 as follows

$$\varepsilon^0: \quad \frac{\partial}{\partial y_i}\left(K_{1ij}^{(0)}\frac{\partial h_1^{(0)}}{\partial y_j}\right) = 0 \qquad \text{in } \Omega_1 \tag{20}$$

$$\varepsilon^0: \quad \left(K_{1ij}^{(0)}\frac{\partial h_1^{(0)}}{\partial y_j}\right)N_i = 0 \qquad \text{on } \Gamma \tag{21}$$

and $h_1^{(0)}$ is **y**-periodic. It can be shown that the solution of the problem (20)-(21) is a function which depends on the macroscopic space variable **x** and does not depend on the local space variable **y** [6, 10, 37],

$$h_1^{(0)} = h_1^{(0)}(\mathbf{x},t^*) = h^{(0)}(\mathbf{x},t^*) \tag{22}$$

It means that the first order solution $h_1^{(0)}$ is constant over Ω_1 and it can be concluded that $h_1^{(0)}$ is a macroscopic variable, which will be denoted $h^{(0)}$. From the water retention curve we also obtain the corresponding water content $\theta_1^{(0)}$

$$\theta_1^{(0)} = h_1^{-1}(h_1^{(0)}) \text{ and inversely } h_1^{(0)} = h_1(\theta_1^{(0)}) \tag{23}$$

2.6. Determination of $h_1^{(1)}$ *and the local boundary value problem*

The local boundary value problem follows from (14) and (17) at the power ε^1

$$\varepsilon^1: \quad \frac{\partial}{\partial y_i}\left[K_{1ij}^{(0)}\left(\frac{\partial h^{(0)}}{\partial x_j}+I_{j3}\right)+K_{1ij}^{(0)}\frac{\partial h_1^{(1)}}{\partial y_j}\right]=0 \qquad \text{in } \Omega_1 \qquad (24)$$

$$\varepsilon^1: \quad \left[K_{1ij}^{(0)}\left(\frac{\partial h^{(0)}}{\partial x_j}+I_{j3}\right)+K_{1ij}^{(0)}\frac{\partial h_1^{(1)}}{\partial y_j}\right]N_i=0 \qquad \text{on } \Gamma \qquad (25)$$

where $h_1^{(1)}$ is **y**-periodic. It can be shown [6,10,37] that the solution of Eqs (24)-(25) can be put in the form of a linear function of the macroscopic gradient $\left(\frac{\partial h^{(0)}}{\partial x_i}+I_{i3}\right)$

$$h_1^{(1)}=\chi_i\left(\frac{\partial h^{(0)}}{\partial x_i}+I_{i3}\right)+\overline{h}^{(1)}(\mathbf{x},t^*) \qquad (26)$$

where each component χ_i of the vector $\boldsymbol{\chi}(\chi_1,\chi_2,\chi_3)$ is a function of the three space coordinates (y_1, y_2, y_3). Moreover, $\boldsymbol{\chi}$ has a zero-valued volume average, which is written

$$\langle\boldsymbol{\chi}\rangle=\frac{1}{|\Omega|}\int_{\Omega}\boldsymbol{\chi}\, d\Omega=0 \qquad (27)$$

In Eq. (26) the term I_{i3} is a component of the identity matrix **I,** while $\overline{h}^{(1)}$ is an arbitrary function of **x** and *t*. The vector $\boldsymbol{\chi}(\mathbf{y})$ is the solution of a classical linear local boundary value problem which is obtained by substituting the solution (26) into the problem (24)-(25) ([6],[10],[36])

$$\frac{\partial}{\partial y_i}\left[K_{1ij}^{(0)}\left(I_{jk}+\frac{\partial \chi_k}{\partial y_j}\right)\right]=0 \qquad \text{in } \Omega_1 \qquad (28)$$

$$K_{1ij}^{(0)}\left(I_{jk}+\frac{\partial \chi_k}{\partial y_j}\right)N_i=0 \qquad \text{on } \Gamma \qquad (29)$$

The vector field $\boldsymbol{\chi}(\mathbf{y})$ characterizes the micro geometry of the period from the point of view of the transfer of water. The solution of the problem (28) and (29) requires information about the microscopic geometry of the porous medium. Except for some particular cases, this problem has to be numerically solved.

2.7. Local flow equation in medium 2

From Eqs. (15) and (16) at the order ε^0 we get the non linear boundary value problem for the capillary pressure head $h_2^{(0)}(\mathbf{x},\mathbf{y},t^*)$ in the domain Ω_2 depending on the local space variable **y**

$$\varepsilon^0: \quad C_2^{(0)} \frac{\partial h_2^{(0)}}{\partial t^*} - \frac{\partial}{\partial y_i}\left(K_{2ij}^{(0)} \frac{\partial h_2^{(0)}}{\partial y_j} \right) = 0 \qquad \text{in } \Omega_2 \qquad (30)$$

$$\varepsilon^0: \quad h_2^{(0)} = h^{(0)} \qquad \text{on } \Gamma \qquad (31)$$

where the conductivity $K_{2ij}^{(0)} = K_{2ij}\left(h_2^{(0)}\right)$ is a function of the capillary pressure head $h_2^{(0)}$. Since $h_2^{(0)}$ is not constant over the sub-domain Ω_2, it can be concluded that local non equilibrium condition is encountered. Thus, we have two capillary pressure head fields, namely $h_1^{(0)} = h_1^{(0)}(\mathbf{x}, t^*)$ and $h_2^{(0)}(\mathbf{x}, \mathbf{y}, t^*)$, interacting each other through the coupling boundary condition (31). This local non-equilibrium is rather complex since the problem (30) and (31) is non linear. Note also that the gravity does not influence the behavior of $h_2^{(0)}$.

2.8. Macroscopic flow model for h^0

In order to determine the macroscopic model let us write Eqs. (14) and (17) at the order $O(\varepsilon^2)$ of approximation:

$$C_1^{(0)} \frac{\partial h^{(0)}}{\partial t^*} - \frac{\partial}{\partial y_i}\left[K_{1ij}^{(0)}\left(\frac{\partial h_1^{(1)}}{\partial x_j} + \frac{\partial h_1^{(2)}}{\partial y_j} \right) + K_{1ij}^{(1)}\left(\frac{\partial h^{(0)}}{\partial x_j} + \frac{\partial h_1^{(1)}}{\partial y_j} \right) + K_{1ij}^{(1)} I_{j3} \right] +$$
$$- \frac{\partial}{\partial x_i}\left[K_{1ij}^{(0)}\left(\frac{\partial h^{(0)}}{\partial x_j} + \frac{\partial h_1^{(1)}}{\partial y_j} \right) + K_{1ij}^{(0)} I_{j3} \right] = 0 \qquad \text{in } \Omega_1 \quad (32)$$

$$\left[K_{1ij}^{(0)}\left(\frac{\partial h_1^{(1)}}{\partial x_j} + \frac{\partial h_1^{(2)}}{\partial y_j} \right) + K_{1ij}^{(1)}\left(\frac{\partial h^{(0)}}{\partial x_j} + \frac{\partial h_1^{(1)}}{\partial y_j} \right) + K_{1ij}^{(1)} I_{j3} \right] N_i = \left[K_{2ij}^{(0)} \frac{\partial h_2^{(0)}}{\partial y_j} \right] N_i \qquad \text{on } \Gamma \quad (33)$$

First, integrate Eq. (32) over the domain Ω_1 and divide it by $|\Omega|$.

$$\frac{1}{|\Omega|}\int_\Omega \left\{ C_1^{(0)} \frac{\partial h^{(0)}}{\partial t^*} - \frac{\partial}{\partial y_i}\left[K_{1ij}^{(0)}\left(\frac{\partial h_1^{(1)}}{\partial x_j} + \frac{\partial h_1^{(2)}}{\partial y_j} \right) + K_{1ij}^{(1)}\left(\frac{\partial h^{(0)}}{\partial x_j} + \frac{\partial h_1^{(1)}}{\partial y_j} \right) + K_{1ij}^{(1)} I_{j3} \right] + \right.$$
$$\left. - \frac{\partial}{\partial x_i}\left[K_{1ij}^{(0)}\left(\frac{\partial h^{(0)}}{\partial x_j} + \frac{\partial h_1^{(1)}}{\partial y_j} \right) + K_{1ij}^{(0)} I_{j3} \right] \right\} d\Omega = 0 \qquad (34)$$

The next four steps concern the transformations of the second term of Eq. (34) and are as follows: (i) apply the Gauss Ostrogradski theorem to transform the volume integral to the surface integral (ii) apply the periodicity condition and the boundary condition Eq. (33); (iii) apply once again the Gauss Ostrogradski theorem to pass from the surface to the volume integral over the domain Ω_2; (iv) make use of Eq. (30). After these transformations we get:

$$\left\langle C_1^{(0)} \right\rangle \frac{\partial h^{(0)}}{\partial t^*} - \frac{\partial}{\partial x_i}\left[K_{1ij}^{(0)} \left(\frac{\partial h^{(0)}}{\partial x_j} + \frac{\partial h_1^{(1)}}{\partial y_j} \right) + K_{1ij}^{(0)} I_{j3} \right] + \left\langle C_2^{(0)} \frac{\partial h_2^{(0)}}{\partial t^*} \right\rangle = 0 \tag{35}$$

where:

$$\left\langle C_1^{(0)} \right\rangle = C^{eff}\left(h^{(0)}\right) = \frac{1}{|\Omega|} \int_{\Omega_1} C_1^{(0)} \, \mathrm{d}\Omega = w_1 C_1^{(0)} \tag{36}$$

is the effective specific water capacity. The volumetric fraction of the medium 1, w_1 [-] is defined as:

$$w_1 = \frac{|\Omega_1|}{|\Omega|} \tag{37}$$

and is of the order O(1). If we use Eq. (36), then the first term in Eq. (35) can be also written as:

$$\left\langle C_1^{(0)} \right\rangle \frac{\partial h^{(0)}}{\partial t^*} = w_1 C_1^{(0)} \frac{\partial h^{(0)}}{\partial t^*} = w_1 \frac{\partial \theta_1^{(0)}}{\partial t^*} = \frac{\partial \theta^{aver}}{\partial t^*} \tag{38}$$

where θ^{aver} [-] is the volumetric water content of the medium 1, averaged with respect to the total volume of the period $\theta^{aver} = w_1 \theta_1^{(0)}$.
The exchange term in Eq. (35) is written as

$$\left\langle C_2^{(0)} \frac{\partial h_2^{(0)}}{\partial t^*} \right\rangle = \frac{1}{|\Omega|} \int_{\Omega_2} C_2^{(0)} \frac{\partial h_2^{(0)}}{\partial t^*} \mathrm{d}\Omega = \frac{1}{|\Omega|} \int_{\Omega_2} \frac{\partial \theta_2^{(0)}}{\partial t^*} \mathrm{d}\Omega \tag{39}$$

Introducing the solution for $h_1^{(1)}$ from Eq. (26) into Eq. (35) leads to the following macroscopic governing equation:

$$C^{eff} \frac{\partial h^{(0)}}{\partial t^*} - \frac{\partial}{\partial x_i}\left(K_{ij}^{eff} \left(\frac{\partial h^{(0)}}{\partial x_j} + I_{j3} \right) \right) + \left\langle C_2^0 \frac{\partial h_2^{(0)}}{\partial t^*} \right\rangle = 0 \tag{40}$$

As we can observe, Eq. (40) has the form of an integro-differential equation. This model contains the gravity term and a source term coming from the interaction with the medium 2. This source term is non linear and requires the solution of the local boundary value problem (30) and (31) over Ω_2. It causes the retardation of the water flow and gives rise to the so-called tailing effect [4]. The same type of model was formerly obtained by Hornung in [21], using a slightly different mathematical methodology.
$\mathbf{K}^{\mathbf{eff}}\left(h^{(0)}\right)$ is the effective conductivity tensor which can be demonstrated to be symmetric and positively definite. It depends on $h^{(0)}$ and $\boldsymbol{\chi}(\mathbf{y})$. Its definition follows from (35) and (26):

$$K_{ij}^{eff}(h^{(0)}) = \frac{1}{|\Omega|}\int_{\Omega_2} K_{ik}^{(0)}\left(\frac{\partial \chi_j}{\partial y_k} + I_{kj}\right)d\Omega \tag{41}$$

The determination of K_{ij}^{eff} requires to solve the local boundary value problem (28)-(29) for $\boldsymbol{\chi}(\mathbf{y})$ over Ω_1 and then to apply the formula (41).
If the local conductivity tensor in the domain Ω_1 is isotropic

$$K_{1ij}^{(0)} = I_{ij}\, K_1^{(0)}$$

then Eq. (41) becomes

$$K_{ij}^{eff} = \frac{1}{|\Omega|}\int_{\Omega_1} K_1^{(0)}\left(\frac{\partial \chi_j}{\partial y_i} + I_{ij}\right)\mathrm{d}\Omega \tag{42}$$

If $K_1^{(0)}$ is constant within the domain Ω_1, than we have

$$K_{ij}^{eff} = \frac{K_1^{(0)}}{|\Omega|}\int_{\Omega_1}\left(\frac{\partial \chi_j}{\partial y_i} + I_{ij}\right)\mathrm{d}\Omega \tag{43}$$

Note that both effective hydraulic parameters, $\mathbf{K}^{eff}(h^0)$ and $C^{eff}(h^0)$ depend on the local parameters of the more conductive domain Ω_1 and on the local geometry.

3. APPLICATION OF THE MODEL

3.1. General strategy of the complete solution of a particular macroscopic boundary value problem

In order to solve a particular boundary value problem one has to follow three main steps: (i) solution of the local boundary value problem (28)-(29) for a given local geometry of the medium; (ii) calculation of the effective parameters $\mathbf{K}^{eff}$ by Eq. (41) and C^{eff} by Eq.(36); (iii) solution of the macroscopic boundary value problem i.e. Eq. (40) together with particular initial and boundary conditions of the problem.
The local boundary value problem concerns an elliptic partial differential equation which can be solved using any commercial code that enables the application of periodic boundary conditions, like for example FEMLAB. To solve the macroscopic problem that has an integro-differential form, a numerical model had to be developed. It is presented in the next section.

3.2 Numerical model of the macroscopic problem

3.2.1 General structure of the numerical model.

The numerical application of the model presented deals with the macroscopically one-dimensional vertical flow problem in a double porosity soil with two- or three-dimensional inclusions, named ***(DPH).*** The algorithm described below was implemented in the Fortran code DPOR_1D developed by the authors.
After replacing the dimensionless variables by the dimensional ones the macroscopic model obtained by homogenization, Eq. (40), can be rewritten as follows:

$$\frac{\partial \theta^{aver}}{\partial t} - \frac{\partial}{\partial X_3}\left(K^{eff}\left(\frac{\partial h}{\partial X_3} + 1 \right) \right) + Q = 0 \tag{44}$$

where θ^{aver} is average water content defined by Eq. (38) and K^{eff} is the effective conductivity in the vertical direction. In this case it is a scalar. Q denotes the source term:

$$Q = \left\langle \frac{\partial \theta_2}{\partial t} \right\rangle \tag{45}$$

The volumetric water content in medium 2, θ_2, is a function of the microscopic variable **y**. In order to determine the value of Q, the local flow problems in all periods should be solved. Due to the continuity of pressure at the interface Γ, the source term Q is a non-linear function of the macroscopic variable h.

For the purpose of numerical solution the mixed (mass-conservative) formulation of unsaturated flow equation proposed by Celia et al. [12] was used. The macroscopic equation is discretized in space by finite differences. The integration in time is performed by fully implicit scheme. The discretized form of Eq. (44) is as follows:

$$\frac{\theta_i^{aver,j+1} - \theta_i^{aver,j}}{\Delta t} - \frac{1}{\Delta x}\left[K_{i+1/2}^{j+1}\left(\frac{h_{i+1}^{j+1} - h_i^{j+1}}{\Delta x} \right) - K_{i-1/2}^{j+1}\left(\frac{h_i^{j+1} - h_{i-1}^{j+1}}{\Delta x} \right) - \left(K_{i+1/2}^{j+1} - K_{i-1/2}^{j+1} \right) \right] + Q_i^{j+1} = 0 \tag{46}$$

where i is the node index, j is the time level index, Δx is the spatial interval (uniform) and Δt is the time step. The interblock conductivities were estimated by arithmetic averages:

$$K_{i\pm1/2} = \frac{1}{2}\left[K^{eff}\left(h_{i\pm1} \right) + K^{eff}\left(h_i \right) \right] \tag{47}$$

Since θ^{aver}, K^{eff} and Q are nonlinear functions of h, at each time level a system of nonlinear equations arises. It was linearized by the Newton method [2], which appeared to be more robust than Picard one, commonly used for typical unsaturated flow problems. The Newton method requires estimation of jacobian matrix in each iteration, which means that derivatives of all terms of the equation should be computed with regard to the macroscopic pressure head which is the main variable. The implicit treatment of source term Q means that its derivative with respect to h should also be computed. This should be done numerically and requires that local flow problems in each period are solved twice. In order to simplify the solution we computed the derivative of Q only for the first iteration in each time step and used the same value in subsequent ones. We found that this significantly reduces the overall computational cost, while maintaining good accuracy of the solution.

Another important issue concerning numerical solution is the time step control. Efficient solution requires variable time step. Usually a simple empirically based algorithm is used, where the size of time step is adjusted according to the number of performed iterations. We found that more rigorous approach based on the estimation of local truncation error can be more robust in case of strongly nonlinear problems. We used an algorithm similar to the one presented in [25], however with the possibility of specifying accuracy in terms of either pressure head or water content.

3.2.2 Solution of the local flow problem in the medium 2.

The local flow problems in the medium 2 can be one-, two- or three-dimensional, according to the geometry of the period. Since we considered simple and regular local geometries (see next section), the finite difference method was used for spatial discretization. In case of two- and three- dimensional problems we used a fractional step method with decomposition of the spatial operator [26]. Each time step was split into three substeps. First, for a given initial value h_i^j, the solution in the y_1 direction is performed, which gives the first intermediate value of $h_i^{j+1/3}$. The intermediate values are used as initial condition for the second substep - solution in the y_2 direction. The corresponding value $h_i^{j+2/3}$ obtained from that second substep is used for the solution in the y_3 direction, which gives the final value h_i^{j+1}. Thus the original 3D problem is replaced by a series of 1D problems for each space direction. This approach considerably speeds up the solution. The additionally introduced error is negligible if the size of time step is sufficiently small.

4. NUMERICAL EXAMPLES

4.1. Description of the test problems

In order to illustrate the presented approach numerical simulations of infiltration into a double-porosity soil were carried out, for two types of geometry.

4.1.2 Geometry and local hydraulic functions

Two different types of local geometry were considered. In example 1 the more conductive regions have the form of vertical columns of square cross section, embedded in less conductive continuous matrix (Fig. 2a). In example 2 the less conductive medium forms horizontal columns of square cross-section (Fig. 2b).
In each case a macroscopic one-dimensional problem was solved for a 50 cm long soil column. The local flow problems are two-dimensional. The volume fractions of the sub domains are nearly equal (w_1 = 0.49 and w_2 = 0.51 in example 1, w_1 = 0.51 and w_2 = 0.49 in example 2).
We assumed that the water retention curve (Fig. 3) and the relative conductivity curve (Fig. 4) were identical in both porous sub-domains, whereas the values of saturated conductivity differed by four orders of magnitude. We used the van Genuchten – Mualem [40] hydraulic functions of the following form:

$$K(h) = K_S \frac{\left\{1 - (\alpha|h|)^{n-1}\left[1 + (\alpha|h|)^n\right]^{-m}\right\}^2}{\left[1 + (\alpha|h|)^n\right]^{m/2}} \tag{48}$$

$$\theta(h) = \theta_R + (\theta_S - \theta_R)\left[1 + (\alpha|h|)^n\right]^{-m} \tag{49}$$

with the following parameters: θ_R = 0.045 cm^3 cm^{-3}, θ_S = 0.430 cm^3 cm^{-3}, α = 0.145 cm^{-1}, n = 2.68, m = 1-1/n = 0.627, which corresponds to the typical sand parameters as given by Carsel and Parrish [11]. The values of saturated conductivities were K_{S1} = 30 cm h^{-1} and K_{S2} = 0.003 cm h^{-1} for medium 1 and 2, respectively.

4.1.3 Effective parameters

The effective parameters were calculated according to Eqs (36) and (43). In example 1 the local boundary problem is one-dimensional and can be analytically solved. For this particular geometry we obtained $K^{eff}(h) = 0.49K_1(h)$. In example 2 the local problem is two-dimensional. It was numerically solved, using FEMLAB. The resulting relation for the effective conductivity was found to be: $K^{eff}(h) = 0.328K_1(h)$ and the effective water retention capacities were $C^{eff}(h) = 0.49C_1(h)$ and $C^{eff}(h) = 0.51C_1(h)$ for example 1 and 2, respectively. The corresponding effective conductivity and retention curves are shown in Figs. 3 and 4, respectively.

4.1.4 Initial and boundary conditions

In example 1 the initial and boundary conditions were assumed to represent the infiltration of water into a dry soil under a prescribed constant flux less than K_{s1}:

h = -1000 cm	-50 cm $\leq x \leq$ 0, $t < 0$
q = 12 cm h^{-1}	$x_3 = 0$, $t \geq 0$

In Example 2, the initial and boundary conditions correspond to the infiltration into dry soil under constant pressure applied at the surface:

h = -100 cm of water	-50 cm $\leq x_3 \leq$ 0, $t < 0$
h = -2 cm	$x_3 = 0$, $t \geq 0$

In both cases, a free drainage was imposed at the bottom of the column:

$\partial h / \partial x_3 = 0$	x_3 = -50 cm, $t \geq 0$

4.2. Comparison of the solutions

For the purpose of comparison for each test problem three different numerical solutions were performed:

1. The fine scale three-dimensional solution (**FS3D**) of the Richards equation in which the heterogeneous structure of the column is exactly represented.

$$C(h)\frac{\partial h}{\partial t} - div_y\left(K(h)grad_y(h + y_3)\right) = 0 \tag{50}$$

The SWMS_3D finite element code developed by Šimůnek et al. [38] was used and the solution was considered as the reference one.

2. The dual porosity model of Gerke and van Genuchten (**DPGG**) [15] where the flow domain is assumed to consist of two continuous overlapping sub domains. The flow in each sub domain is described by the Richards equation. The equations are coupled by a first-order exchange term:

$$w_1 C_1(h_1)\frac{\partial h_1}{\partial t} - div_x\left(w_1 K_1(h_1) grad_x(h_1 + x_3)\right) + Q = 0 \quad (51)$$

$$w_2 C_2(h_2)\frac{\partial h_2}{\partial t} - div_x\left(w_2 K_2(h_2) grad_x(h_2 + x_3)\right) - Q = 0 \quad (52)$$

where the indices 1 and 2 refer to the medium 1 and 2, respectively. The water exchange term Q has the following form:

$$Q = \frac{\beta}{a^2}\gamma K_a(h_a)(h_1 - h_2) \quad (53)$$

where β [-] is a geometry dependent coefficient, a is the distance from centre to surface of low permeable block of medium 2, γ [-] is an empirical coefficient and K_a is the conductivity of the interface between medium 1 and 2, defined as a function of the average pressure at the interface h_a. The interface conductivity K_a was evaluated from the following formula:

$$K_a = 0.5\left(K_a(h_1) + K_a(h_2)\right) \quad (54)$$

We assumed that the function K_a (h) is equal to the conductivity of low permeable medium K_2 (h). In example 1 the following values of parameters were used: γ = 0.4, a = 0.75 cm and β = 2.82, whereas in example 2 γ = 0.4, a = 0.175 cm and β = 11. The value of β was chosen following the suggestions presented in [15].
The numerical solution of the DPGG model was obtained using our own Fortran code with the corresponding finite difference discretization scheme and the Picard iterative method.

3. The single porosity model (**SP**), where the less conductive domain is completely inactive (no flow and no water exchange with the more conductive domain).

$$C^{eff}(h)\frac{\partial h}{\partial t} - div_x\left(K^{eff}(h) grad_x(h + x_3)\right) = 0 \quad (55)$$

The solution was obtained using the DPOR_1D **(DPH)** code with the exchange term set to zero.

4.3. Treatment of the boundary conditions

The flux imposed at the soil surface in example 1 represents mean value averaged over the cross section of the soil surface. It was assumed that the whole amount of water infiltrates into the more conductive medium 1 (medium 2 is effectively sealed at the surface). Thus, for the DPGG solution we imposed local infiltration rates q_1 = 12/0.49 = 24.49 cm h^{-1} in medium 1 and q_2 = 0 in medium 2. Similarly, in the FS3D solution with SWMS_3D code we imposed infiltration rate equal to 24.49 cm h^{-1} only on the part of surface occupied by medium 1 and flux was set to zero on the other part.

4.4. Numerical parameters

In example 1 all numerical solutions were performed using uniform spatial discretization in x_3 direction (Δx = 0.25 cm). The discretization of 2D local flow problems in y_1 and y_2 direction for the DPOR_1D solution was uniform (0.125 cm), whereas for the SWMS_3D solution the spatial interval varied from 0.0625 cm to 0.125 cm. In example 2 the SP, DPGG and DPH solutions were obtained with Δx = 0.5 cm. In the DPH solution each node corresponds to one inclusion. Each inclusion was discretized with Δy = 0.0175 cm. Due to the symmetry, the local problem is solved in a quarter of inclusion only. In case of fine scale solution we used variable spatial discretization with spatial step ranging from 0.0025 to 0.06 cm for each direction. All calculations were performed with variable time step, with the initial value being as small as 10^{-12} h. The real time of the numerical simulation varies considerably for different models. For the SP and the DPGG solutions it is of the order of a few seconds, for the DPH approach - several hours and for the FS3D solution - up to 100 hours (all calculations were performed on comparable machines)

4.5. Results and discussion

4.5.1. Example 1

The evolution of the mean capillary pressure head in medium 1 at the bottom of the column is shown in Fig. 5. The mean capillary pressure head corresponds to the macroscopic capillary pressure for DPH and SP solutions, while for DPGG solution it corresponds to h_1 in medium 1. In FS3D solution it is calculated as an average over the part of cross section surface occupied by medium 1. It can be seen that the DPH gives a solution very close to the fine scale solution (FS3D). The evolution of the capillary pressure head in the DPGG model is slightly different.
The time evolution of the flux at the bottom of the column is presented in Fig. 6. The presence of the low conductive medium 2 slows down the propagation of wetting front, which is clearly visible. The homogenized solution (DPH) is nearly the same as the 3D reference solution (FS3D). The DPGG approach produced a different solution. In that case the arrival of the wetting front is faster, but later on the flux takes longer time to reach a steady state. This difference can be clearly explained by comparing the values of the source term in the DPGG and DPH models. The time evolution of these terms at different depths in the column is shown in Fig. 7. We also provided the water exchange rates obtained in FS3D solution, calculated as the variation of water content in medium 2 over time. It can be seen that the water transfer rate in the DPGG model is significantly underestimated during the initial phase of infiltration, while during later stages of the process it is slightly overestimated. This problem was also shown by Gerke and van Genuchten [16].
The flux in the double porosity soil reaches its steady state value considerably later compared to the single porosity example. This retardation, known as the tail effect, can be estimated by the normalized tail flux q_T defined as:

$$q_T = \frac{q_S - q_D}{q_S} \tag{56}$$

where q_S and q_D are the fluxes calculated from the simple porosity and double porosity models (DPH, DPGG or FS3D, respectively). Thus, the value of q_T varies between 0 and 1, which indicates minimum and maximum value of the tail effect. Fig.

8 presents the evolution of q_T at the bottom of the column with respect to time t_R. which represents the time of appearance of the non zero flux in the single porosity model (SP).

4.5.2. Example 2

The evolution of the mean capillary pressure head in medium 1 is presented in Fig. 9 and the evolution of the mean flux at the bottom of the column is presented in Fig 10. The slower propagation of the wetting front in the double porosity medium can be easily observed, as it was in example 1. The solution obtained from the DPGG approach is significantly different from the others. This can be partially explained by the fact that the estimation of the effective macroscopic conductivity of medium 1 in the DPGG model is based on the volume fraction of medium 1 only. As a result the steady state flux corresponding to given boundary conditions is about 50% greater than the one obtained with the other solutions. The small discrepancy between the steady state flux obtained by DPH and FS3D calculations can be explained by numerical factors (different methods of spatial discretization and grid sizes).
The time evolution of the exchange term along the column is shown in Fig 11. Again, the values from DPH, DPGG and FS3D models are compared. Note that the DPH solution is close to the reference solution, while the DPGG gives results that are very different qualitatively and quantitatively. The normalized tail flux q_T as a function of the time t_R is presented in Fig 12. In that case the negative values obtained from the DPGG solution are due to the fact that the macroscopic flux in this model is considerably larger than that obtained from the single porosity approach.

5. CONCLUSIONS

A macroscopic model (mathematical and numerical) of water flow in unsaturated double porosity soils was presented, based on the homogenization approach. The model consists of a single integro-differential equation with two effective hydraulic parameters. It was found that the macroscopic behavior is governed by the capillary pressure head in the more conductive and connected sub domain. Non equilibrium of the capillary pressure prevails locally in such media. This non equilibrium is attributed to the contrast in the hydraulic parameters of the two sub-domains of the double porosity soil. The model is valid if the scale separation exists and the contrast between the hydraulic diffusivities of the two sub-domains is of the order $O(\varepsilon^2)$, which means $O(\varepsilon^3) << D_2 / D_1 << O(\varepsilon)$. The effect of the “double porosity” in the macroscopic governing equation was taken into account through an exchange term which represents the coupling between the microscopic and the macroscopic scales. This term causes the retardation of the water flow (tailing effect) with respect to the simple porosity medium in which the less conductive domain was considered as completely impermeable. When the hydraulic diffusivities are less contrasted, the local equilibrium model is applicable [27].

It was shown that the effective hydraulic parameters depend on the parameters of the more conductive sub domain and the local geometry of the medium. The effective hydraulic parameters can be easily calculated if the local hydraulic parameters of the more conductive domain and the local geometry of the medium are known.

The numerical simulations showed that the double porosity model gives the results close to the fine scale solution, which was considered as the reference solution within the capillary flow physics (the Richards equation). For a simple local geometry (example 1), the Gerke and van Genuchten phenomenological model gave results for mean capillary pressures and fluxes close to the double porosity model obtained from the present homogenization approach. This is valid, despite of the poor approximation of the exchange term at short times. In the case of a more complex local geometry (example 2), the comparison between the Gerke and van Genuchten model and the double porosity homogenization model showed very different results. The differences observed can be explained by an inadequate in this case estimation of the effective hydraulic conductivity and the source term proposed in the Gerke and van Genuchten model.

We are aware that the model presented here should be experimentally validated. Since the experimental data in double-porosity soils are very scarce and/or are not fully exploitable for that purpose, experiments are currently being carried out, under controlled laboratory conditions, and will be published in a forthcoming paper, when completed.

It should also be emphasized that the work presented in this paper is related to the problem of the preferential water flow in soils. It is just a matter of vocabulary. One can consider the more conductive medium as a source of an enhanced flow (preferential flow) or the less conductive medium as a cause of retardation of the flow. The latter point of view was chosen in the paper.

ACKNOWLEDGMENTS

This research was founded by the French PNRH program, through the project « Transferts complexes en milieu poreux et ressources en eau ». The French Ministry of Foreign Affaires and the Region Rhône-Alpes (MIRA program) are greatly acknowledged for their scholarships to A. Szymkiewicz. The calculations were performed partially at MIRAGE (Grenoble, France) and CI TASK (Gdańsk, Poland).

REFERENCES

[1] Amaziane B., Bourgeat A., Koebbe J. Numerical simulation and homogenization of two-phase flow in heterogeneous porous media. Transport in Porous Media 1991; 6 (5-6): 519-547

[2] Arbogast T. Computational aspects of dual-porosity models. In: Hornung U. (ed.). Homogenization and porous media. New York : Springer-Verlag, 1997.

[3] Arbogast T., Douglas J.Jr., Hornung U. Derivation of the double porosity model of single phase flow via homogenization theory. SIAM J. Math. Anal. 1990; 21: 823-836.

[4] Auriault J.-L., Effective macroscopic description for heat conduction in periodic composites, Int. J. Heat Mass Transfer 1983; 26: 861-869.

[5] Auriault, J.-L. Heterogeneous medium. Is an equivalent macroscopic description possible ? Int. J. Engng Sci. 1991; 29(7): 785-795.

[6] Auriault J.-L., Lewandowska J. Diffusion non lineaire en milieux poreux. C.R. Acad. Sci. Paris, 1997, t. 324, série II b: 293-298.

[7] Barenblatt G.I., Entov V.M., Ryzhik V.M. Theory of fluid flows through natural rocks. Kluwer, 1990.
[8] Barenblatt G.I., Zheltov I.P., Kochina I.N. Basic concepts in the theory of seepage of homogeneous liquids in fissured rocks. P.M.M. 1960; 27(2): 348-350.
[9] Bear, J. Dynamics of Fluids in Porous Media, Elsevier, 1972.
[10] Bensoussan, A., Lions J.-L., Papanicolaou, G. Asymptotic analysis for periodic structures, North-Holland, 1987.
[11] Carsel R.F., Parrish R.S. Developing joint probability distributions of soil water retention characteristics. Water Resour. Res. 1988; 24(5):755-769.
[12] Celia M.A., Bouloutas E.T., Zarba R.L. A general mass-conservative numerical solution for the unsaturated flow equation. Water Resour. Res. 1990; 26(7):1483-1496.
[13] Dane J.H., Topp G.C. (ed.) Methods of Soil Analysis, Part 4 - Physical Methods, Soil Science Society of America, 2002.
[14] Durner W. Hydraulic condutivity estimation for soils with heterogeneous pore structure. Water Resour. Res. 1994; 30: 211-233.
[15] Gerke H.H., van Genuchten M.Th. A dual-porosity model for simulating the preferential movement of water and solutes in structured porous media. Water Resour. Res. 1993; 29(2):305-319.
[16] Gerke H.H., van Genuchten M.Th. Evaluation of a first-order water transfer term for variably saturated dual-porosity flow models. Water Resour. Res. 1993; 29(4):1225-1238.
[17] Gerke H.H., van Genuchten M.Th. Macroscopic representation of structural geometry for simulating water and solute movement in dual-porosity media. Adv. Water Resour. 1996; 19(6):343-357.
[18] Germann P.F. Kinematic wave approach to infiltration and drainage into and from soil macropores. Trans. ASAE 1985; 28: 745-749.
[19] Germann P.F., Beven K. Kinematic wave approximation to infiltration into soils with sorbing macropores. Water Resour. Res. 1985; 21(7): 990-996.
[20] Gwo J.P., Jardine P.M., Wilson G.V., Yeh G.T. A multiple-pore-region concept to modeling mass transfer in subsurface media. J. of Hydrol. 1995; 164 : 217-237.
[21] Hornung U. Homogenization of miscible displacement in unsaturated aggregated soils. In: Dynamical systems, St. Petersburg, 1991.
[22] Hornung U. (ed.). Homogenization and porous media. New York : Springer-Verlag, 1997.
[23] Hornung U., Showalter R.E. Diffusion models for fractured media. J. Math. Anal. Appl. 1990; 147: 69-80.
[24] Jarvis N.J. The MACRO model (version 3.1). Technical description and sample simulations. Reports and Dissertations 19. Department of Soil Science, Swedish University of Agricultural Science, Uppsala, Sweden, p.51,1994.
[25] Kavetski D., Binning P., Sloan S.W. Adaptive time stepping and error control in a mass conservative numerical solution of the mixed form of Richards equation. Adv. Water Resour. 2001; 24:595-605.
[26] Le Pourhiet A.Numerical solution of partial differential equations (in French). Toulouse : Cepadues Editions, 1988.

[27] Lewandowska J., Laurent J.-P. Homogenization modeling and parametric study of moisture transfer in an unsaturated heterogeneous porous medium. Transport in Porous Media 2001; 45: 321-345.
[28] Mohanty B.P., Bowman R.S., Hendrickx J.M.H., van Genuchten M.Th. New piecewise-continuous hydraulic functions for modeling preferential flow in an intermittent flood-irrigated field. Water Resour. Res. 1997; 33: 2049-2063.
[29] Panfilov M. Macroscale models of flow through highly heterogeneous porous media. Kluwer Academic Publishers, 2000.
[30] Quintard M., Cherblanc F., Whitaker S. Dispersion in heterogeneous porous media: One-equation non-equilibrium model. Transport in Porous Media 2001; 44(1): 181-203.
[31] Quintard M., Whitaker S. One-phase flow in porous media: Effects of local heterogeneities (in French). J. Méca. Theorique et Appliquée 1987; 6(5): 691-726.
[32] Quintard M., Whitaker S. Two-phase flow in heterogeneous porous media: The method of large scale averaging. Transport in Porous Media 1988; 5: 341-379.
[33] Richards L.A. Capillary conduction of liquids through porous medium. Physics, 1931, 1, 318-333.
[34] Ross P.J., Smettem K.R. A simple treatment of physical nonequilibrium water flow in soils. Soil Sci. Soc. Am. J. 2000; 64: 1926-1930.
[35] Royer P., Auriault J.L., Boutin C. Macroscopic modeling of double-porosity reservoirs. J. Petr. Sci. Enging. 1996; 16: 187-202.
[36] Saez A.E., Otero C.J., Rusinek I. The effective homogenous behavior of heterogenous porous media. Transport in Porous Media 1989; 4: 213-238.
[37] Sanchez-Palencia, E., Non-homogeneous media and vibration theory. Lecture Note in Physics, 127, Springer-Verlag, Berlin, 1980.
[38] Šimůnek J., Huang K., van Genuchten M.Th. The SWMS_3D code for simulating water flow and solute transport in three-dimensional variably-saturated media. Version 1.0. Research Report No. 139, U.S. Salinity Laboratory, Riverside, California, 1995.
[39] Šimůnek J., Jarvis N.J., van Genuchten M.Th., Gärdenäs A. Review and comparison of models for describing non-equilibrium and preferential flow and transport in the vadose zone. J. of Hydrol. 2003, 272: 14-35.
[40] van Genuchten M.T. A closed form equation for predicting the hydraulic conductivity of unsaturated soils. Soil Sci. Soc. Am. J. 1980; 44: 892-898.
[41] Warren J.R. , Root P.J. The behavior of naturally fractured reservoirs. Soc.of Petro. Eng. J.1963; Sept.: 245-255.

LIST OF SYMBOLS

Latin letters

a	the characteristic size of the less permeable inclusion (in DPGG model)[L]
C_1, C_2	specific water capacity [L^{-1}]
C^{eff}	effective specific water capacity [L^{-1}]
C_1^*,C_2^*	dimensionless specific water capacity [-]
D	hydraulic diffusivity [$L\ T^{-2}$]
h_1,h_2	capillary pressure head in medium 1 and 2 [L]
h_1^*,h_2^*	dimensionless capillary pressure head [-]
$\boldsymbol{I}$	identity matrix
$\mathbf{K}$	hydraulic conductivity tensor [$L\ T^{-1}$]
K_a	hydraulic conductivity of the interface (in DPGG model) [$L\ T^{-1}$]
K^{eff}	effective hydraulic conductivity [$L\ T^{-1}$]
K_{s1}, K_{s2}	hydraulic conductivity at saturation of medium 1 and 2 [$L\ T^{-1}$]
$\mathbf{K}^*$	dimensionless hydraulic conductivity tensor [-]
L	characteristic macroscopic length [L]
l	characteristic microscopic length [L]
m	water retention function parameter (in van Genuchten model) [-]
$\mathbf{N}$	unit vector normal to the surface Γ
n	water retention function parameter (van Genuchten model) [-]
Q	exchange term [T^{-1}]
t	time [T]
t_R	retardation time [T]
t^*	non-dimensional time [-]
T	characteristic time [T]
w_1,w_2	volumetric fractions of medium 1 and 2 [-]
$\mathbf{X}$	dimensional space variable [L]
$\mathbf{x}$	macroscopic dimensionless space variable [-]
$\mathbf{y}$	microscopic dimensionless space variable [-]

Greek letters

α	water retention function parameter (van Genuchten model) [L^{-1}]
β	parameter (in DPGG model) [-]
Γ	interface between medium 1 and 2
γ	parameter (in DPGG model) [-]
Δt	time step [T]
Δx	space interval [L]
ε	scale separation parameter [-]
θ_1, θ_2	volumetric water content [-]
θ^{aver}	average volumetric water content [-]
$\boldsymbol{\chi}$	vector function, solution of the local boundary value problem [-]
Ω	period
Ω_1, Ω_2	domains of the period occupied by medium 1 and 2

Acronyms:

DPH	Double Porosity Homogenization Model
DPGG	Dual Porosity Model of Gerke and van Genuchten
FS3D	Fine Scale 3D Model
SP	Single Porosity Model

LIST OF FIGURES

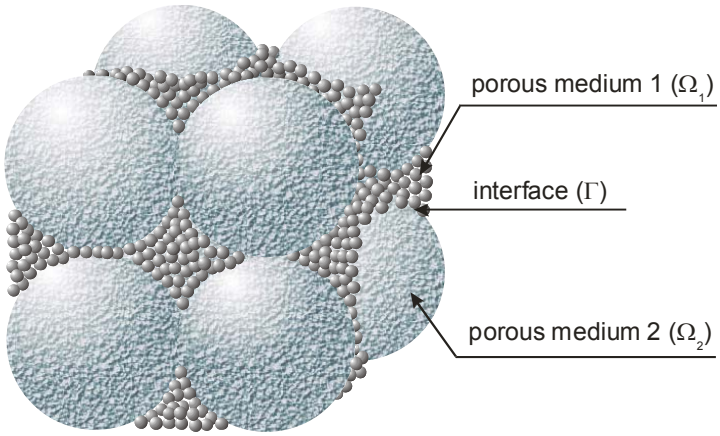

Fig. 1. Structure of double porosity medium

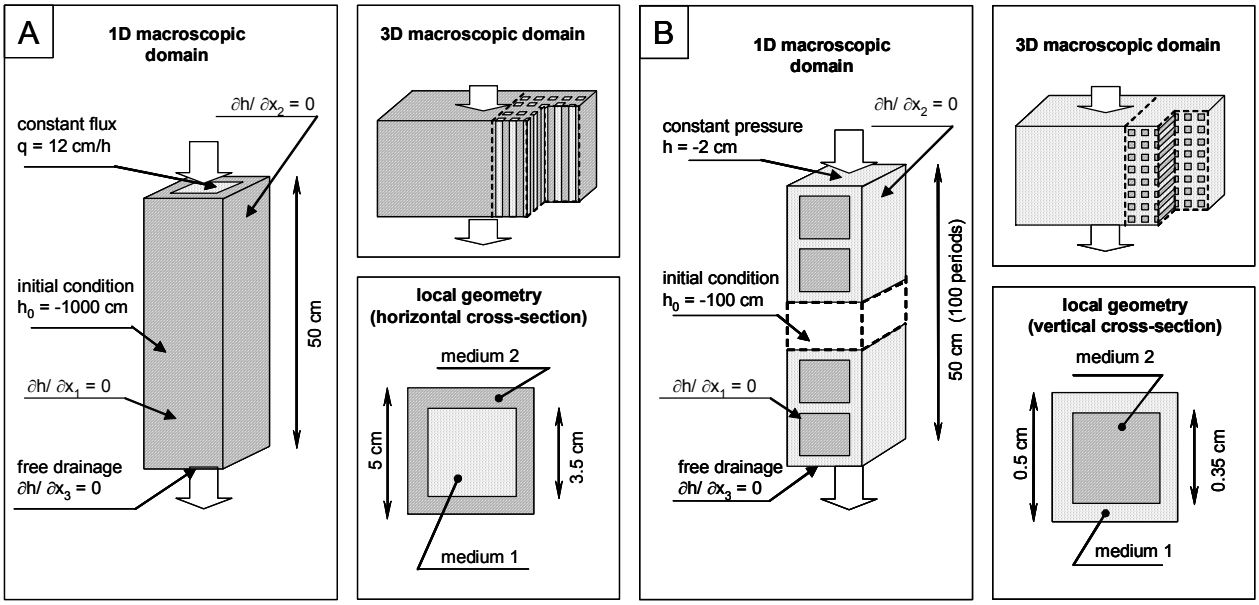

Fig. 2. Geometry of double porosity medium and boundary conditions used in numerical tests: A) example 1, B) example 2

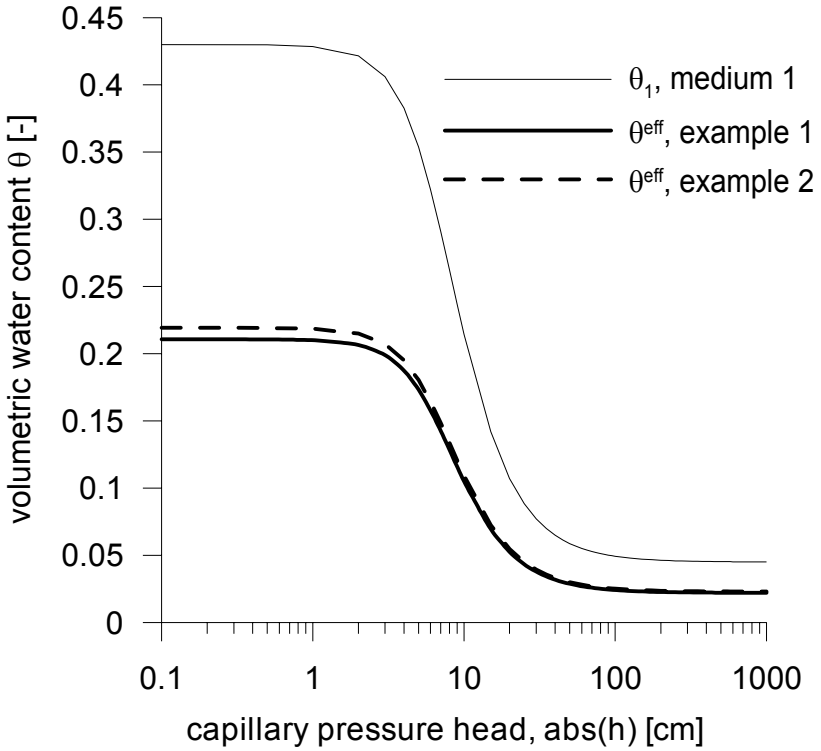

Fig. 3. Water retention function of medium 1 ($\theta_1(h)$) and effective water retention functions ($\theta^{ever}(h)$) used in numerical examples

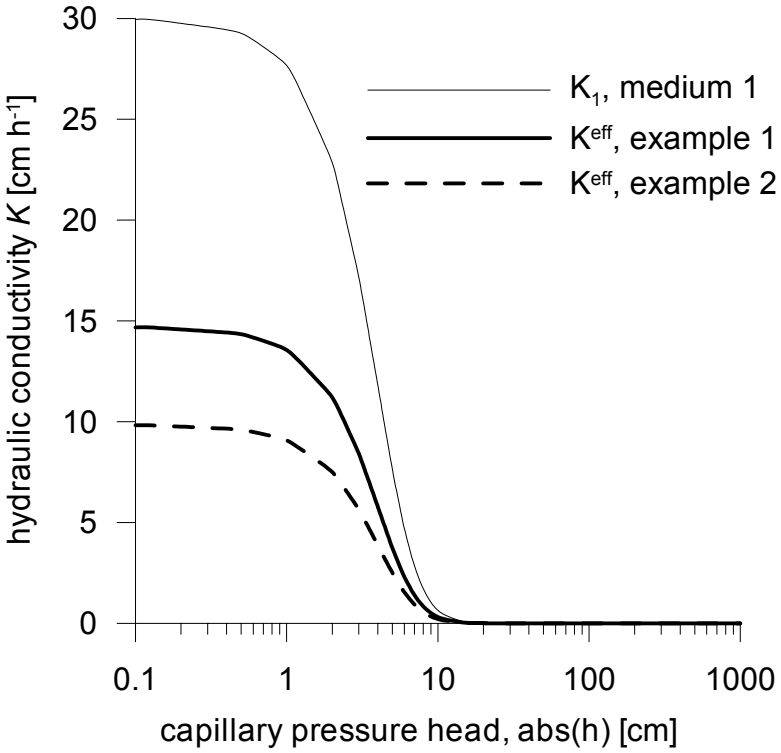

Fig. 4. Hydraulic conductivity of medium 1 ($K_1(h)$) and effective conductivity ($K^{eff}(h)$) used in numerical examples

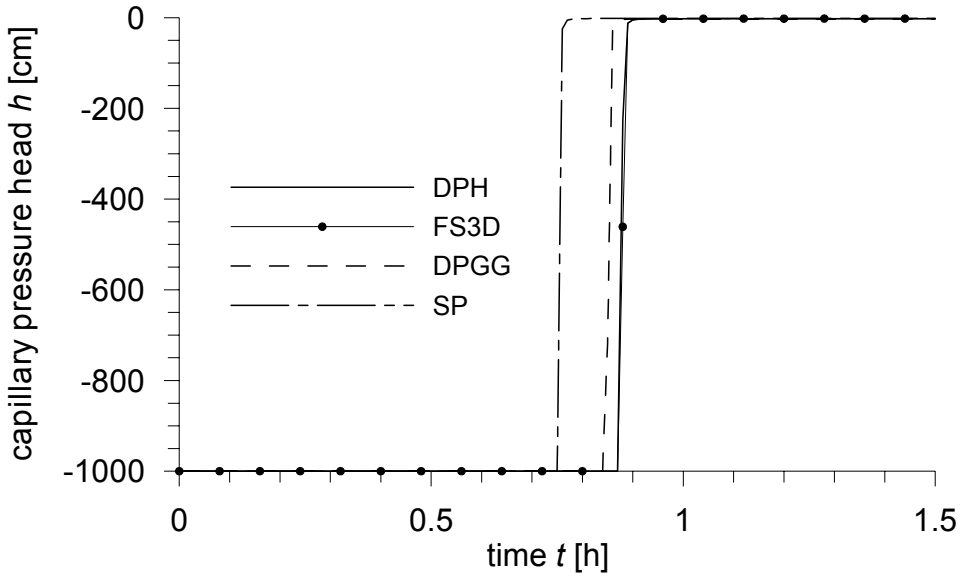

Fig. 5. Example 1: Evolution of the mean capillary pressure head in medium 1 at x_3 = -50 cm according to the model obtained by homogenization (DPH), the reference solution (FS3D), the Gerke and van Genuchten (DPGG) and the simple porosity (SP) approaches

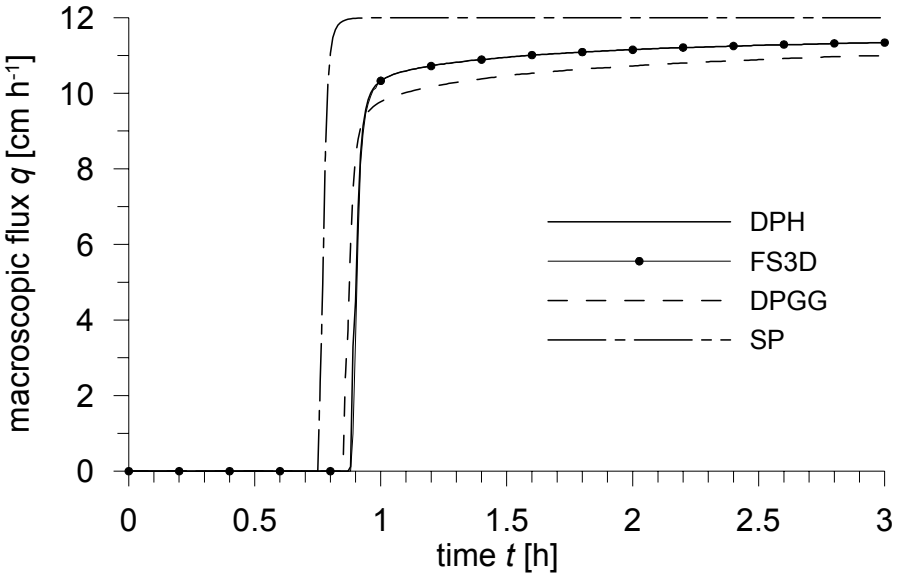

Fig. 6. Example 1: Evolution of the macroscopic flux q at x_3 = -50 cm according to the model obtained by homogenization (DPH), the reference solution (FS3D), the Gerke and van Genuchten (DPGG) and simple porosity (SP) approaches

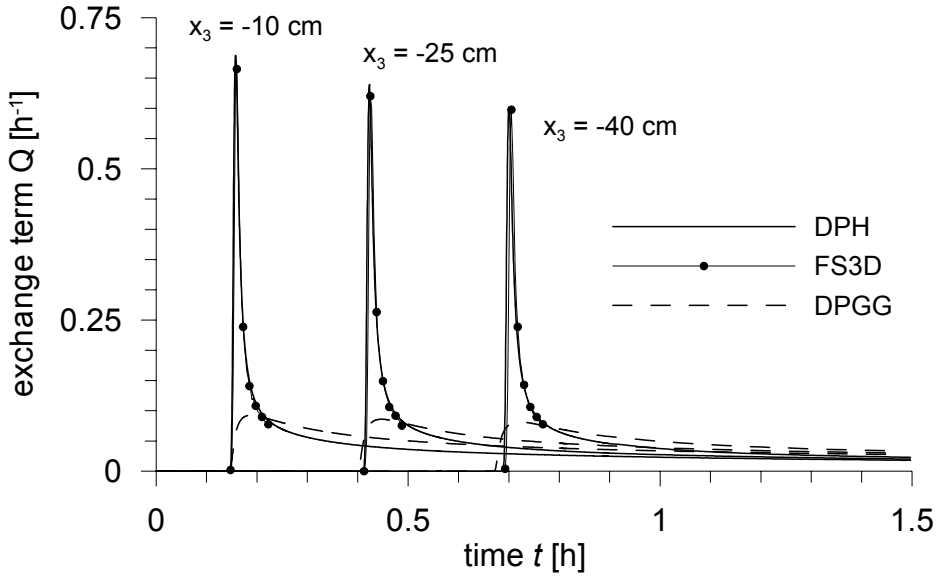

Fig. 7. Example 1: Evolution of the exchange term Q at different depth of the column according to the model obtained by homogenization (DPH), the reference solution (FS3D) and the Gerke and van Genuchten model (DPGG)

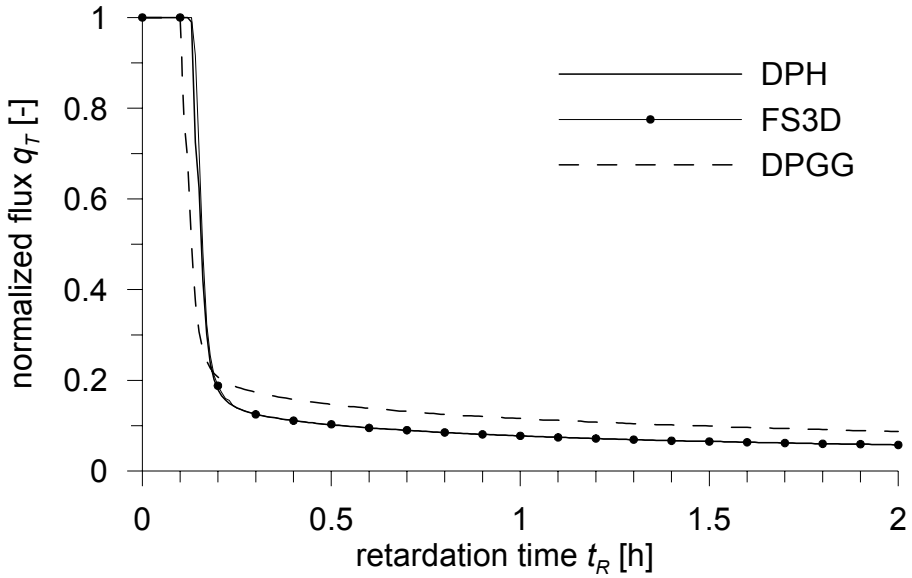

Fig. 8. Example 1: Evolution of the normalized tail flux q_T at x_3 = -50 cm according to the model obtained by homogenization (DPH), the reference solution (FS3D) and the Gerke and van Genuchten model (DPGG); q_T is the relative difference between the flux in simple (SP) and double (DPH, DPGG and FS3D) porosity models; the retardation time t_R = 0 corresponds to the arrival of wetting front in the simple porosity model.

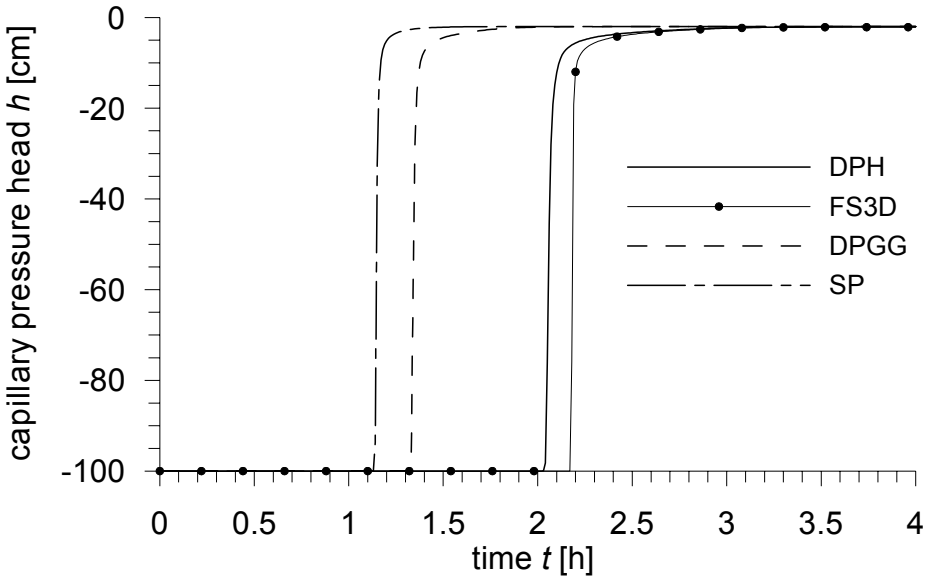

Fig. 9. Example 2: Evolution of the mean capillary pressure head in medium 1 at x_3 = -50 cm according to the model obtained by homogenization (DPH), the reference solution (FS3D), the Gerke and van Genuchten model (DPGG) and the simple porosity model (SP)

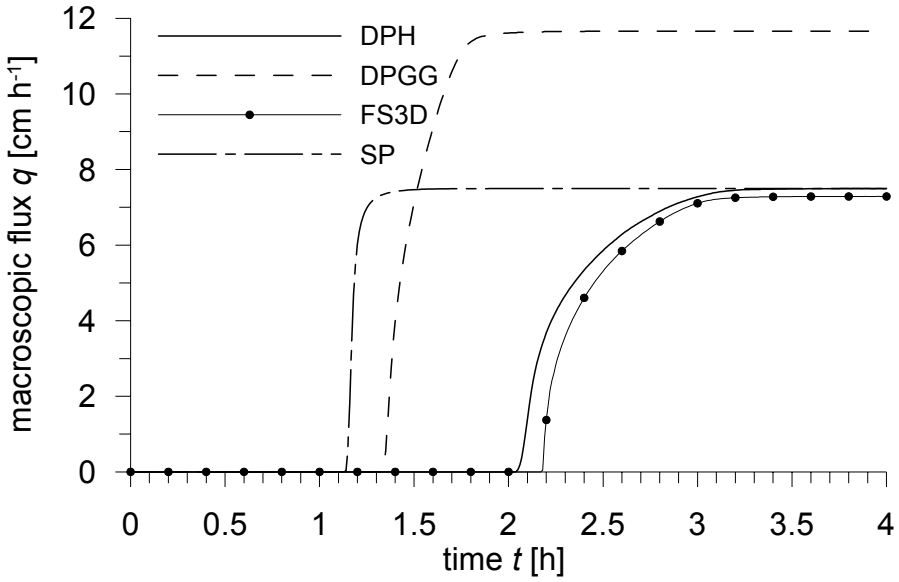

Fig. 10. Example 2: Evolution of mean flux q at x_3 = -50 cm according to the model obtained by homogenization (DPH), the reference solution (FS3D), the Gerke and van Genuchten (DPGG) model and the simple porosity model (SP)

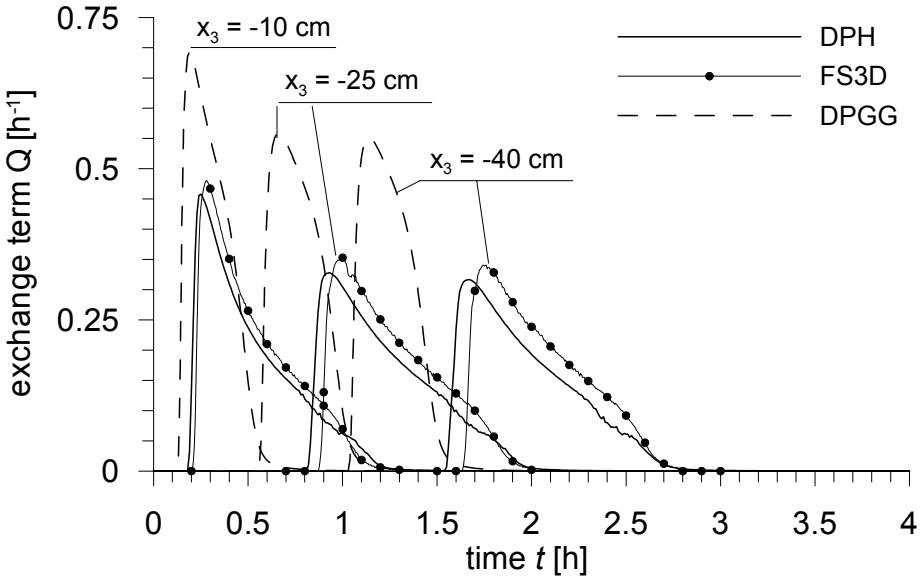

Fig. 11. Example 2: Evolution of the exchange term Q at different depths of the column according to the model obtained by homogenization (DPH), the reference solution (FS3D) and the Gerke and van Genuchten model (DPGG)

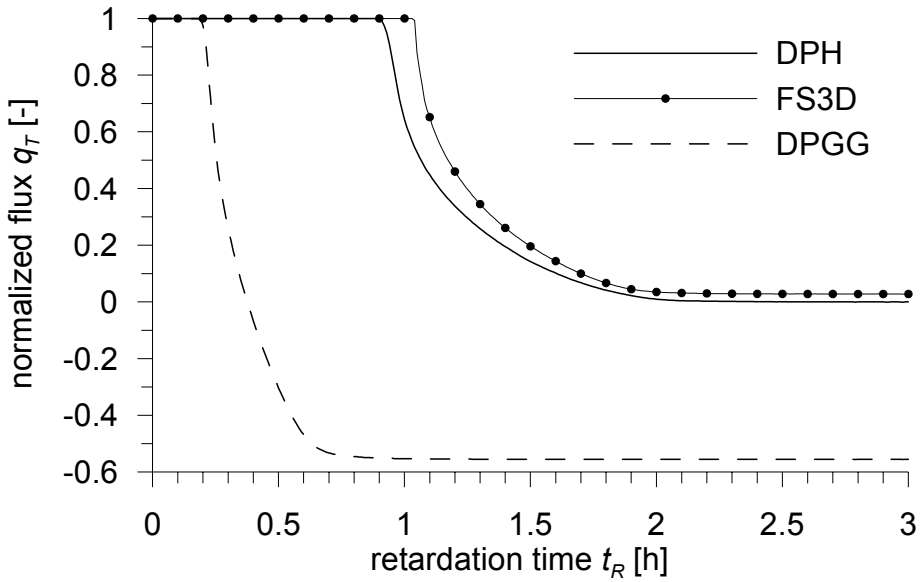

Fig. 12. Example 2: Evolution of the normalized tail flux q_T at x_3 = -50 cm according to the model obtained by homogenization (DPH), the reference solution (FS3D), and Gerke and van Genuchten model (DPGG); q_T is the relative difference between the flux in simple (SP) and double (DPH, DPGG and FS3D) porosity models; the retardation time t_R = 0 corresponds to the arrival of wetting front in the simple porosity model